ELASTIC-PLASTIC ANALYSIS OF CRACKS IN PIPE

K.Kaddouri, B.Bachir Bouaidjra, M.Belhouari and K.Madani
Department of Mechanical Engineering, University of Sidi Bel Abbes,
BP 89, Cité Ben M'hidi , Sidi Bel Abbes, 22000, Algeria.
E-Mail : kaddourikacem@yahoo.fr

Abstract

Fracture analysis of pipes with circumferential cracks is an important task for leak-before-break characteristics. This paper presents elastic and elastic-plastic finite element solutions of J-integral for pipe containing cracks under pressure. This analysis is based on a three-dimensional non-linear finite element method with small strain theory. The effects of different parameters were analysed such as: crack dimensions, loading and hardness coefficient.

1. Introduction

Pressure vessels and pressure piping used in refineries, chemical processing plants, water treatment systems of boilers, low pressure storage tanks commonly used in process, pulp and paper and electric power plants operate over a broad range of pressures and temperatures and experience a variety of operating environments. Shell, head, attachments, and piping are some of the components that commonly fail. One of the most important common types of failure is cracking [1-4]. The study of the crack behaviour in theses kinds of structures is then very important to predict the lifespan. Since Rice [5], The J integral is the most used criteria for analysing the fracture behaviour of ductile materials and the J integral may be determined analytically, numerically or experimentally . With the development of the power computing, the finite element method gives with a very good accuracy the values of the J integral at the crack front in for ductile materials. Several works interested to the pipe crack subjected to tensile load and bending [2,4]. The aim of the present study is to analyse, by the finite element method, the behaviour of semi-elliptical pipe cracks under pressure for elastic and elastic-plastic material by determining the J integral at the crack front. They analysis were performed for pipe with different radius-to-thickness ratio, and for various position

2. Geometrical and material models:

Let's consider a cylindrical surface with semi-elliptical surface crack. Two position of the crack were studied (fig. 1). The dimension of the crack is defined by the half-length c and the depth a. The material was selected to be power law hardening with an elastic –plastic behaviour characterized by the Ramberg-Osgood stress-strain relationship:

$$\frac{\varepsilon}{\varepsilon_o} = \frac{\sigma}{\sigma_o} + \alpha\left(\frac{\sigma}{\sigma_o}\right)^n \qquad (1)$$

Where: α is the Ramberg-Osgood factor, n the power law-hardening exponent, ε_0. is the yield strain and σ_0. is the yield stress.

This material law is in effect a non-linear elastic law and can be applied to a power plastic material under conditions of proportional loading (Deformation plasticity theory). This model

employs a representation of the uniaxial (tensile) stress-strain curve consisting of two parts: an initial, linear response followed by a pure power law model. The model supports only a small-strain formulation. The assumptions of purely proportional loading in the model are questionable at best when finite strains large rotations of material elements occur. Using an effective stress (σ_0) defined from the von Mises yield function and an effective strain (e) defined from the Prandlt-Reuss relations, the total stress components in term of the total stain components are given by :

$$\frac{\sigma_{ij}}{\sigma_0} = \frac{1}{3(1-2\nu)}\frac{\varepsilon_{kk}}{\varepsilon_0}\delta_{ij} + \frac{2}{3}\frac{\sigma_e/\sigma_0}{e_e/\varepsilon_0}\frac{e_{ij}}{\varepsilon_0} \qquad (2)$$

Where the effective stress and strain are defined by:

$$\sigma_e^2 = \frac{1}{2}\left[(\sigma_{11}-\sigma_{22})^2 + (\sigma_{22}-\sigma_{33})^2 + (\sigma_{33}-\sigma_{11})^2 + 6(\sigma_{12}^2+\sigma_{23}^2+\sigma_{13}^2)\right]$$

$$e_e^2 = \frac{9}{2}\left[(\varepsilon_{11}-\varepsilon_{22})^2 + (\varepsilon_{22}-\varepsilon_{33})^2 + (\varepsilon_{33}-\varepsilon_{11})^2 + \frac{3}{2}(\gamma_{12}^2+\gamma_{23}^2+\gamma_{13}^2)\right]$$

Wide ranges of configuration parameters are considered. They are all combination of the following ratios: crack surface length to thickness of the pipe a/t=0.4, 0.6, 0.7, 0.8, and 0.9; crack surface length to depth a/c=0.25, 0.4, 0.6 and 0.8;

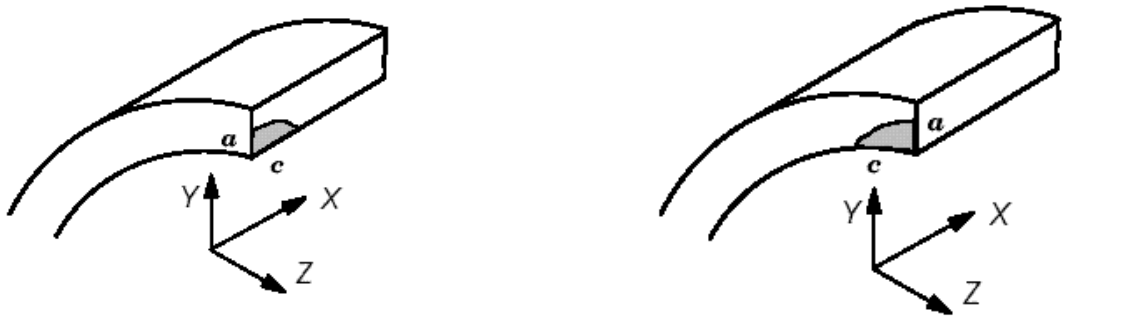

(A) Longitudinal Surface Crack (B) Transverse Surface Crack

FIGURE 1. Geometrical model: position A and B.

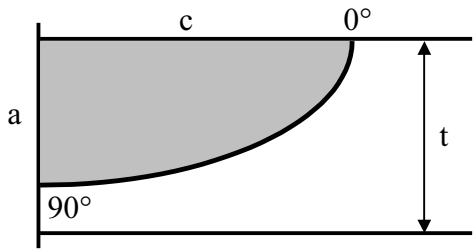

FIGURE 2. Elliptical surface of crack.

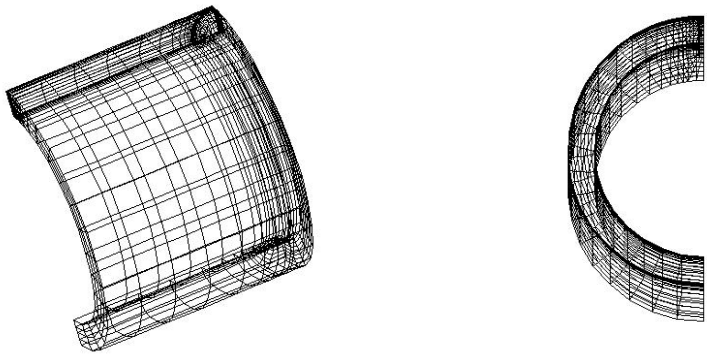

FIGURE 3. Typical mesh model: position A and B.

3. Finite Element analysis

3.1. Creation of Finite Element mesh:

The three dimensional 3D Finite Element mesh for the geometrical model were generated using WARP3D code developed at university of Illinois [6-8]. The model consists of solid brick elements of 8-nodes. In WARP3D the model is divided into three zones. In each region node and element numbering is controlled by three indices in a systematic way, making it easy to locate specific nodes and elements in the different parts of model. This simplifies the definition of the boundary conditions and application of external loading.

The mesh in focused region is formed by ellipses and hyperbolas by use of conformal mapping. The coordinates can be evaluated according to

$$X = \beta (\rho + 1/\rho) \cos \varphi \quad (3)$$

$$Y = \beta (\rho - 1/\rho) \sin \varphi \quad (4)$$

Where: β is scaling factor determined by the crack geometry as:

$$\beta = \frac{1}{2}\sqrt{c^2 - a^2}$$

Thus, the sides of the elements coincide with constant values of either ρ or φ (Fig.2). For different combinations of wide ranges, the WARP3D generate a mesh model that contains between 3606 and 6385 nodes for 2891 and 5250 8-node hybrid brick elements. Fig. 3 show typical mesh model for the two position of the crack.

3.2. J-Integral formulation

A local value of the mechanical energy release rate, denoted J(s), at each point s on a planar, non growing crack front under general dynamic loading is given by:

$$J=\lim_{\Gamma\to 0}\int_{\Gamma}\left[W_S n_1 - P_{ji}\frac{\partial u_i}{\partial X_1}n_j\right]d\Gamma \qquad (6)$$

Where: W_s is the stress-work density per unit volume at $t_i=0$; Γ is a vanishing small contour which lies in the principal normal plane at s, and n_1 is the unit vector normal to Γ . P_{ji} denotes the non-symmetric 1st Piola-Kirchhoff stress tensor which is work conjugate to the displacement gradient expressed on the $t_i=0$ configuration. $\partial u_i/\partial X_j$: the stress-work rate is simply $P_{ji}\partial u_i/\partial X_j$ per unit volume at $t_i=0$. All field quantities are expressed in the local orthogonal coordinate system, x,y,z at locations on the crack front.

All proposed forms of path independent integrals for application in fracture mechanics derive from Eq.(6) by specialization of the loading and material behaviour. Moran and Shih [10,11] have proven the local path independence of J on the actual shape of Γ.

The quantity J defined by Eq.(6) has no direct relationship to the form of the near-tip strain-stress fields, except for very limited circumstances. For plane-stress and plane-strain conditions, with nonlinear elastic material response and small-strain theory, J of Eq.(6) simplifies to the well-known J integral due to Rice [5] that exhibit global path independence.

The role of J as a single parameter which characterizes the near tip strain-stress fields for arbitrary loading. The stress-work density (W_s) per unit initial volume may be defined in terms of the mechanical strains as:

$$W_S = |F|\int_0^{t_i}(t_C : d)\,dt_i \qquad (7)$$

Where $|F|$ denotes the determinant of the deformation gradient $F=\partial x/\partial X$, t_c denotes the unrotated Cauchy stress and d is the unrotated rate of deformation tensor computed from displacements gradients.

4. Result and discussions

Fig.4 shows the distribution of the J-integral along the crack front for elastic behaviour (n=1) for different values of a/t and c/a=4. It can be seen that the J-integral increase with the increase of a/t. The crack extension lead a higher dissipation of energy. It can be also seen in fig. 1 that the J integral is higher at $\varphi=0$. In this position, the radius of curvature is minimum. The crack will propagates in the c direction (longitudinal direction of the pipe).

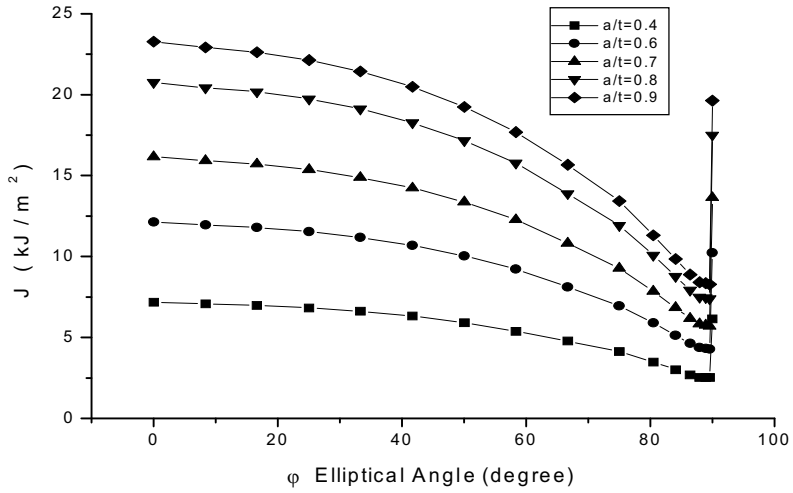

FIGURE 4. Distribution of the J integral along the crack front for n=1, Position A

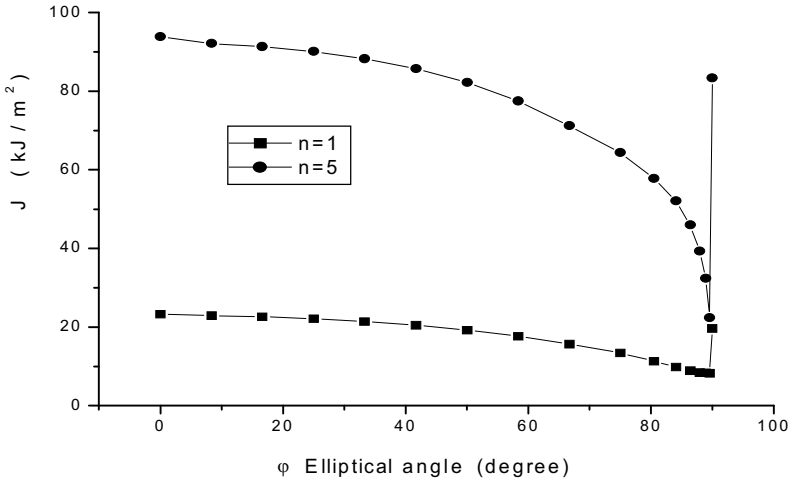

FIGURE 5. Distribution of the J integral along the crack for n=1 and n=5 Position A.

Fig 5 presents a comparison of the J-integral distribution between a elastic (n=1)and elastic-plastic (n=5). It is noted that there is a same trending for elastic behaviour but the value of the J-integral of the elastic-plastic behaviour are larger. In order to confirm this conclusion, it is plotted in fig .6 the value of the J-integral at $\varphi = 0°$ as a function of the applied for n=1 (elastic) and n=5 (elastic-plastic). It is noted that for weak values of the applied pressure there is not a great difference between the elastic J and elastic-plastic J, and for a higher values of the applied pressure the difference is some significant. One can explain the difference by the fact that, for weak pressure there is not a significant plastic work near the crack front and the elastic J integral is appreciably equal to the plastic one.

For high-applied (Fig.6) pressure the plastic work increase with the increase of the pressure ad the plastic component of the J-integral increase too. Wich explain the high difference of the elastic J-integral and elastic-plastic J-integral at high-applied pressure.

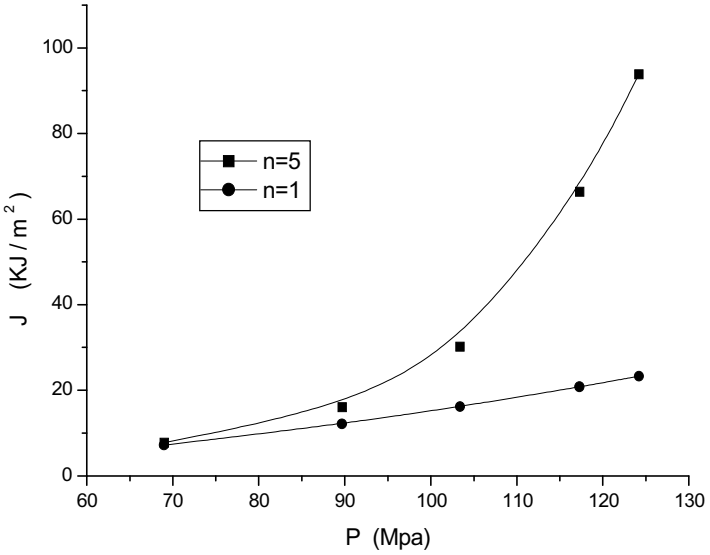

FIGURE 6. Variation of the J integral for different pressure

Position A.

Fig. 7 illustrates a the distribution of J integral for the two orientations of the cracks: longitudinal and transversal cracks. It can be noted that longitudinal cracks present a high values of the J integral compared with the transversal one, and the difference is important at the extremities of the crack (φ=0° and φ=90°). This behaviour can be explained by the fact that a longitudinal crack is subjected to elevated stress, because the applied pressure is normal to the cylinder surface. The mode I opening crack is than more important for a longitudinal crack.

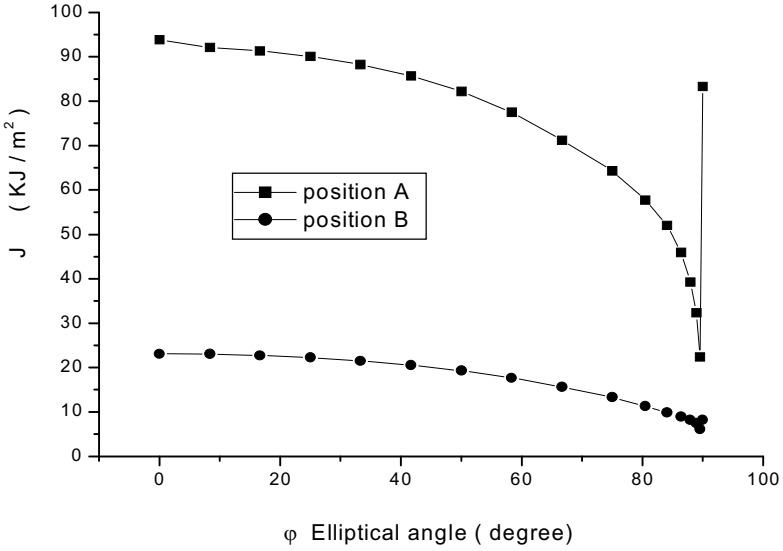

FIGURE 7. Distribution of the J integral along the crack front for crack

Orientations A and B (n= 5 , c/a=4).

5. Conclusion

In this paper, three dimensional, elastic and elastic-plastic, finite element analyses for two orientations of cracks in pipe are studies. The following conclusions can be drawn from the present analysis:

- The study of the variation of the J integral along the contour of the crack showed that the value is maximum for the smallest curvatures radius.

- The value of the J integral is larger as the a/t ratio increases.

- The value of the J integral J is larger for the elastic-plastic behaviour compared with the elastic one.

- The value of the J integral is more important for the longitudinal cracks.

References

1. Firmature, R. and Rahman, S.,*Engineering Fracture Mechanics* , vol. **66**, 15-39, 2000.

2. Rahman, S. and Wilkowski, G., *Engineering Fracture Mechanics*, vol. **61**, 191-211, 1998.

3. Brust,F.W., Rybicki, E.F., *Journal of Pressure Vessel Technology*, Vol. **103**, 226-232, 1981.

4. Yun-Jae, K., Nam-Su, H. and Young-Jim, K. *International Journal of Fracture*, vol. **111**, 71- 86, 2001.

5. Rice, J., *J. of App.Mech*., vol. **35**, 379-386.

6. Gullerud, A.S., Koppenhoefer, K.C., Roy, A and Dodds Jr, R.H., *University of Illinois at Urbana-Champaign,* 2000.

7. Koppeenhoefer, K., Gullerud, A., Ruggieri, C., Dodds, R., and Healy B., *Structural research Series (SRS) 596,* University of Illinois at Urbana-Champaign 1999

8. Gullerud, A., Gao, X., Dodds, R., and Haj-Ali, R., *Eng Fract Mech*, vol.**66**, 65-92, 2000

9. Moran, B and Shih C.F., *Int. J. Frac. Mech*., vol. **35**, 295-310, 1987.

10. Moran, B and Shih C.F., *Engng .Fract .Mech*., vol. **27**, 615-642, 1987.